The Structure-Phase State and Corrosion Resistance Modification of Austenitic Steel in Various Conditions Ion Implantation

S.V. Ovchinnikov*, A.N. Tyumentsev*, A.D. Korotaev**, O.I. Nalesnik***, Yu.P. Pinzhin*, A.G. Nikolaev****, G.Yu. Yushkov****

* *Institute of Strength Physics and Material Science, Siberian Division, Russian Academy of Sciences, Akademicheskii pr. 2/1, Tomsk, 634050, Russia 382-2 531569, osv@spti.tsu.ru*
** *Siberian Institute of Physics and Technology, Novosobornaya pl. 1, Tomsk, 634050, Russia*
*** *Tomsk Polytechnic State University, Lenina pr. 30, 634050, Russia*
**** *High Current Electronics Institute, Siberian Division, Russian Academy of Sciences, Akademicheskii pr.4, Tomsk, 634055, Russia*

With the purpose of an experimental justification of new methods for the improvement of the operational properties of the cans of fuel elements (FE's) of nuclear reactors with the use of implanters such as MEVVA and TITAN a complex examination of the features of modification of the microstructure and corrosion behavior of the surface of type 02X17H14M2 steel in the course of ion implantation (II) has been performed. The features of the phase and structural transformations of ion-doped layers have been revealed depending on the structural state of the target, the type of ions, the vacuum medium of the implanter, and the irradiation dose. It has been shown that the ion implantation with yttrium and titanium ensures a considerable decrease in corrosion rate and precludes the development of intercrystallite corrosion (ICC) of the steel during heat treatments imitating the phase-structure transformations under the service conditions of FE's. The conditions have been revealed and specific modes for enhancement of the corrosion resistance of the test steel by II have been developed. An analysis of the most probable mechanisms for such an enhancement has been carried out.

As follows from the literature data [1–3, 4], when FEs made of austenitic stainless steels are operated in water-moderated reactors their lifetime is determined by the processes developing on the surface of contact with the heat carrier, such as various types of corrosion in the active medium of the heat carrier, nucleation and development of surface cracks, intergranular fracture, irradiation creep, etc. Therefore, there are strong grounds for believing that under these conditions some methods of surface treatment applied to FEs can be used effectively to increase their lifetime since they aimed at appropriate changing the composition, the structure-phase state, and the properties of grain boundaries.

Of considerable promise in this respect are ion-beam and ion-plasma methods for surface treatment, e. g., ion implantation showing practically limitless possibilities for ion doping (including with elements immiscible with the target material either in the solid or in the liquid state) and for the formation in the surface layers of a broad spectrum of structural states (amorphous, nanophase, amorphous-crystalline, etc.) [5–7].

In view of the foregoing, the research program of this paper is aimed at upgrading the performance of austenitic-stainless-steel FEs used in water-moderated reactors (in high-parameter water). A method to be used for the surface modification of FEs is ion implantation.

The physical principles to be used in choosing the type of implanted elements and the modes of ion-beam treatment are dictated by the needs:

1) to enhance the corrosion resistance of the surface layer and, first of all, its resistance to intercrystalline corrosion;

2) to increase the cohesive strength of grain boundaries and to moderate the tendency to nucleation and propagation of intercrystalline cracks;

3) to enhance the stability of austenite in the near-boundary zones;

4) to prevent the solid solution in these zones from being depleted of chromium as a result of the segregation of chromium carbides.

In our opinion, the above effects can be attained by ion-beam doping of the surface layers with Cr, Ni and highly active elements such as Y, or Ti.

Investigations were performed with type 02X17H14M2 steel (Fe – 16.8% Cr – 14.1% Ni – 2.1% Mo – 1% Mn, – 0.007%C, – 0.04%Si, – 0.01%S, – 0.009%P, – 0.001%B, wt.%). The samples used were in three structural states:

I. Deformed ($\varepsilon \approx 70\%$) by rolling to plates of thickness 0.3 mm.

II. Deformed by rolling in the above way and recrystallized at 1273 K for one hour, the resulting grain size being about 30 μm.

III. Recrystallized and then mechanically polished.

Investigations were performed on MEVVA and TITAN implanters with the use of ions of Y, Ti, Ni + Cr. The rate of dose buildup (controlled by varying the pulse repetition rate) was chosen such that the sample temperature increased by no more than $\Delta T \approx 30°$. The II modes are presented in Table 1. The basic characteristic used to estimate the efficiency of the ion-beam

Table 1. Ion implantation modes. (The pressure in the implanter chamber was (2–4)·10^{-6} Torr.)

II mode	Ion species	Irradiation dose, cm^{-2}	Accelerating voltage, kV	Average current density, $\mu A/cm^2$	Target temperature, K
I	Ni+Cr	$1.5 \cdot 10^{17}$	50	9	≤ 320
II	Y	10^{16}	50	9	≤ 320
III	Y	$2.5 \cdot 10^{16}$	50	9	≤ 320
IV	Ti	10^{16}	50	9	≤ 320
V	Ti	$2.5 \cdot 10^{16}$	50	9	≤ 320

treatment is the material resistance to intercristalline corrosion measured before and after surface treatment as well as after sensitizing annealings of untreated and treated specimens. The electrochemical behavior of the steel was studied with the help of a type P-5848 potentiostat. The investigations were carried out in a three-electrode cell of volume 200 ml with the use of an auxiliary platinum electrode and a reference chlorosilver electrode. After measuring the corrosion potential, the anode or cathode polarization curve was tapped off with the potential varied linearly toward the anode or cathode side from the corrosion potential [8, 9].

1. Effect of Ion Implantation on the Microstructure of Austenitic Stainless Steel

Implantation of nickel and chromium ions

Electron microscopy has shown that after ion implantation of these species (irradiation dose $D \approx 1.5 \cdot 10^{17}$ cm^{-2}) into samples being in structural state III a substructure is formed in the surface layer in which the following structural components can be distinguished: (1) ultrafine-grained γ-austenite with a rystallite size of about 0.1 μm that had been formed in the process of mechanical polishing; (2) the same phase in the nanocrystalline state (Fig. 1), and (3) a structural state which can be identified as amorphous or subnanocrystalline (with a crystallite size of some fractions of a nanometer). For samples being in structural state II, ion implantation leads to the formation of a substructure with a high density of chaotically distributed dislocations and small-angle boundaries of misorientation. For both of the above states no second phase segregates are observed. Dispersed particles of second phases with sizes from a few to several tens of nanometers (Fig. 2) are detected in doped samples after annealing at $T = 1273$ K and 923 K. Electron diffraction analysis has shown that these segregates can be identified as complex oxides of the $FeCrNiO_x$ type. They arise as the result of formation, in the course of ion implantation, of nonequilibrium solid solutions of oxygen in the lattice of γ-austenite. Annealing at $T = 1273$ K following ion implantation also leads to recrystallization of the surface layer. The average grain size in this case is ~30 μm like for the unaffected (undoped) samples subjected to annealing under the same conditions.

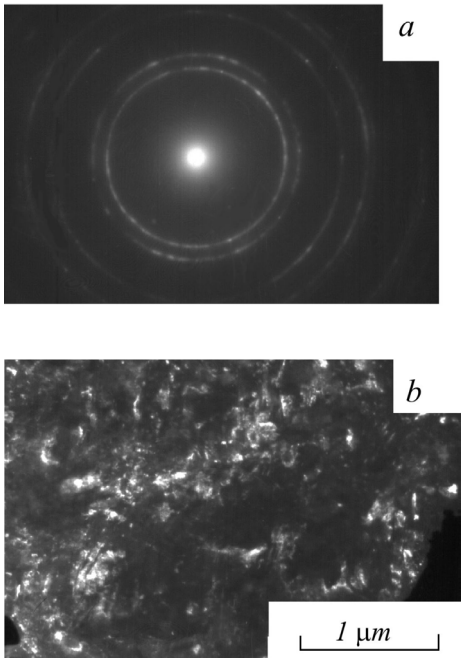

Fig. 1. Electron diffraction pattern (*a*) and dark-field image (*b*) of nanostructured γ-Fe layer after Ni + Cr ion implantation at a dose of $1.5 \cdot 10^{17}$ cm^{-2} in a vacuum $2 \cdot 10^{-6}$ Torr

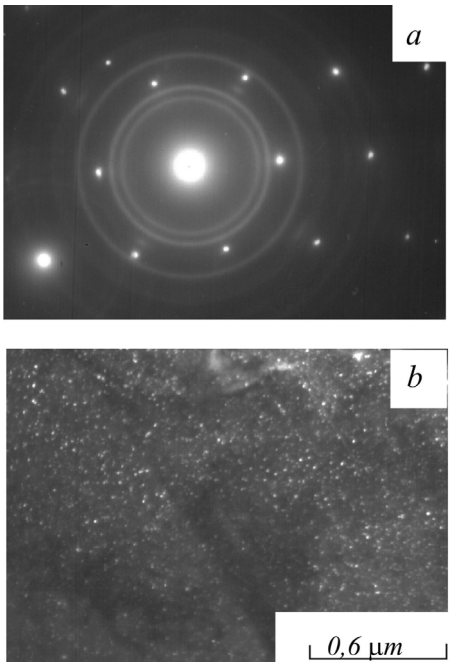

Fig. 2. Electron diffraction pattern (*a*) and $FeCrNiO_x$ particles (*b*) after Ni + Cr ion implantation (see Fig. 1) and subsequent annealing at 1273 K for 1 h

Implantation of Y and Ti ions

It has been established that for all treatment modes presented in Table 1, the modification of the element composition and structural state of the surface layer in the process of II and subsequent post-implantation

annealings at 1273 K shows the following qualitatively similar features:

ion implantation of yttrium and titanium ions ($D \approx 10^{16}$ and $2.5 \cdot 10^{16}$ cm^{-2}), like implantation of nickel and chromium, has no effect on the phase composition of the surface layers. The structural modification of the latter reduces to an only increase in dislocation density. Yttrium and titanium forms nonequilibrium substitutional solid solutions in the lattice of γ-austenite;

highly dispersed (10–200 nm in diameter) particles of the second phase are formed (Fig. 3) only in the process of annealing at 1273 K, being in the main oxides of implanted elements (Y_2O_3 and TiO_2) and carbides of these elements in insignificant amounts;

the above particles show high thermal stability and are segregated predominantly at dislocations, small-angle boundaries of the substructure, and at grain boundaries(Fig. 3,*a*);

in the surface layers with a well-developed defect substructure (structural states I and III), this results in efficient suppression of recrystallization (Fig. 3,*c*) and in a decrease in grain size (by a factor of 1.5–2).

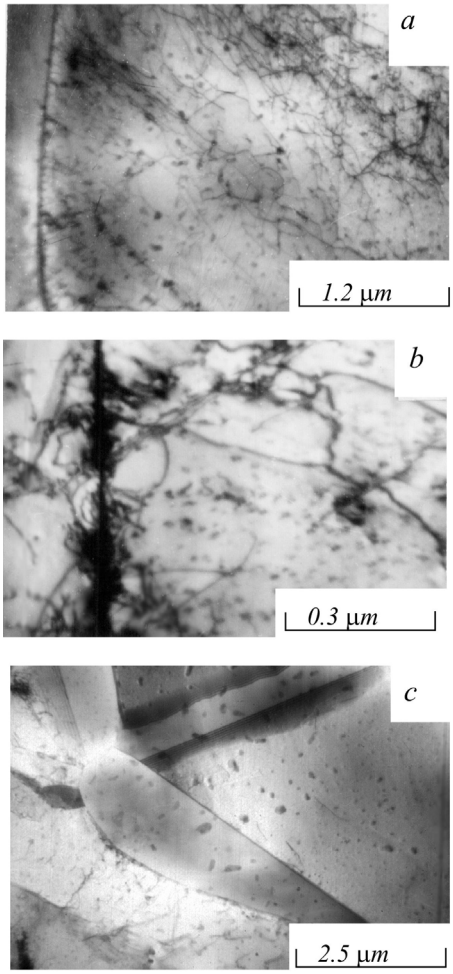

Fig. 3. Microstructure of the surface layer after ion implantation and subsequent annealing at 1273 K for 1 h.
Implanted elements: Y (*a*) and Ti (*b, c*)

2. Influence of Ion Implantation on the Corrosion Resistance of the Steel

Influence of heat treatment on the corrosion resistance of the steel in initial state

The study performed has shown that after annealing at 1273 K the steel is in a passive state and her the steady-state potential is strongly shifted toward the positive side from the equilibrium natural potential. The principal components of the test steel (iron, chromium, and nickel) have the following steady-state potentials in solutions of their salts: –0.44, –0.74, and –0.25 V, respectively. The average corrosion potential of the test steel in 0.5 M H_2SO_4 is +0.37 V, which confirms its state of passivity.

Plotting the polarization curves jointly in the coordinates $\lg i = f(E)$ allows one to find the exchange current at the corrosion potential. Analysis of these curves has shown that the corrosion rate of the test steel after annealing at $T = 1273$ K is $1 \cdot 10^{-6}$ A/cm^2 or 0.011 mm/year.

The annealing at $T = 923$ K, imitating phase transformations at grain boundaries during the operation of FE's reduces the corrosion potential to –0.24 V. The anode polarization curve has thus a portion of rising current which seems to correspond to an intense oxidizing of the metal. As a result the exchange current or the corrosion rate increase substantially, the latter reaching $5.6 \cdot 10^{-6}$ A/cm^2 or 0.061 mm/year, which is a factor of 5.6 higher than the corrosion rate estimated after annealing at $T = 1273$ K (Table 2).

Corrosion resistance of steel after ion implantation

The ion implantation of nickel and chromium does not increase the resistance of the test steel to intercrystallite corrosion. This seams to be related to the high density of oxides segregated in the ion- doped layer in the process of past-implantation annealings.

The most important results have been obtained in investigating the corrosion resistance of the steel doped with yttrium and titanium ions. Immediately after yttrium ion implantation at a radiation dose $2.5 \cdot 10^{16}$ cm^{-2}, the steady-state corrosion potential shifts toward the region of negative voltages ($E_{st} = -0.26$ V). Analysis of electron microscopy data has shown that the reduction in corrosion resistance in this case might be related to the increased electrochemical activity of the surface layer as a result of the formation of highly equilibrium solid solutions of yttrium and oxygen in the fcc lattice of γ-austenite and due to the high internal stresses localized at grain boundaries. Thermal treatment of samples at 1273 K for 1 h, resulting in decay of oversaturated solid solutions (with segregation of yttrium carbide and oxide particles) and relaxation of internal stresses in the ion-doped layer, regain the steady-state corrosion potential to 0.4 V. The anode and cathode polarization curves (see Fig. 4) appear to be similar in shape to those observed for the steel in the original state (without II).

Table 2. Influence of heat treatment and ion implantation on the corrosion resistance of steel 02X17H14M2

No.	Structural state	Final annealing temperature, K	Corrosion rate		Corrosion rate ratio
			A/cm^2	mm/year	
1	Original	1273	$1\cdot10^{-6}$	$1.1\cdot10^{-2}$	100%
2	After II with Y	1273	$1.41\cdot10^{-7}$	$1.5\cdot10^{-3}$	14%
3	After II with Ti	1273	$8.3\cdot10^{-8}$	$9.1\cdot10^{-4}$	8.2%
4	Original	923	$5.6\cdot10^{-6}$	$6.1\cdot10^{-2}$	100%
5	After II with Y	923	$1.9\cdot10^{-7}$	$2.1\cdot10^{-3}$	3.4%
6	After II with Ti	923	$9.5\cdot10^{-8}$	$1.1\cdot10^{-4}$	1.7%

The anode current also slowly increases by the linear law as the potential is increased to 0.9 V, after which oxygen starts releasing. The cathode polarization curve also has a small peak at a potential of 0.32 V. The difference is that the exchange current decreases. The corrosion rate (see Table 2) is $1.41\cdot10^{-7}$. Additional annealing at 923 K for an hour caused some decrease in corrosion potential (from 0.4 to 0.13 V). The steel however remained in a passive state, which is testified by the anode curve (see Fig. 5) having no peak in the region of intense oxidation as contrasted to the original steel annealed in the same mode. The exchange current of the yttrium-doped steel subjected to additional annealing slightly increased and was $1.9\cdot10^{-7}$ A/cm^2. The corrosion rate (see Table 2) was thus 0.0021 mm/year, that is after the annealing provoking phase transformations in FE cans it increased only by 25%. The above value of corrosion rate is 29 times lower than that of the steal in the original state (without II) after a provoking annealing at $T = 923$ K and 5.5 times lower than that estimated for the samples annealed at $T = 1273$ K.

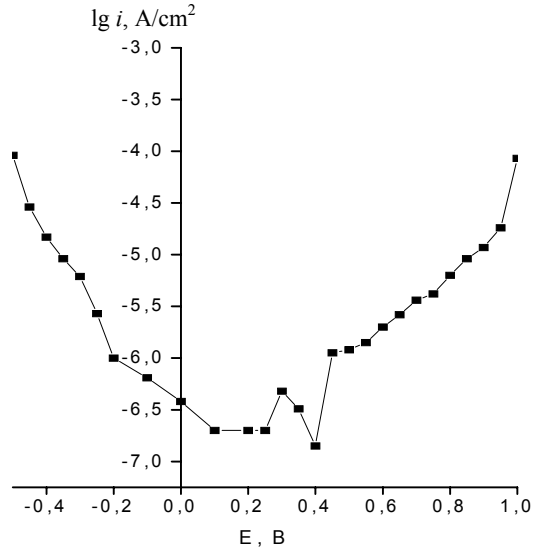

Fig. 4. The polarization curves of steel 02X17H14M2 implanted with yttrium at a dose of $2.5\cdot10^{16}$ cm^{-2} and subse quently annealed at 1273 K for 0.5 h

After ion implantation of the steel with titanium at a dose of $2.5\cdot10^{16}$ cm^{-2} and subsequent annealing at $T = 1273$ K the corrosion potential of the steel is 0.22 V and the main portions of the anode and cathode polarization curves are linear, indicating that the steel is in a passive state for the potential range from –0.20 to +0.85 V. The polarization curves plotted have allowed us to find the exchange current equal to $8.3\cdot10^{-8}$ A/cm^2, which corresponds to a corrosion rate of 0.0009 mm/year (Table 2). Annealing at $T = 923$ K resulted in a slight decrease in corrosion potential (from 0.22 to 0.15 V). This corresponds to an increase in corrosion rate by 14.4%: $i = 9.5\times10^{-8}$ A/cm^2 or 0.00104 mm/year.

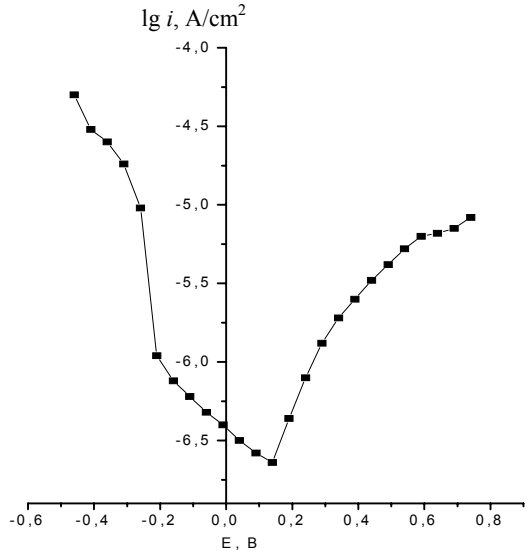

Fig. 5. The polarization curves of steel 02X17H14M2 implanted with yttrium at a dose of $2.5\cdot10^{16}$ cm^{-2} and subse quently annealed at 1273 K for 0.5 h and at 923 K for 1 h

The above values of the corrosion rate are 58 times lower than those estimated for the steel in the original state (without II) after provoking annealing at $T = 923$ K and 12 times lower than the corresponding values for samples annealed at $T = 1273$ K. Comparison with the above data on the ion implantation with yttrium (see Table 2) indicates that the ion implantation with titanium appears to be a more efficient method of increasing the corrosion resistance of the test steel.

Thus, the ion implantation of the steel with yttrium and titanium not only precludes a decrease in corrosion resistance of the steel during provoking heat treatments at 923 K, but provides its considerable increase as compared to the corrosion resistance of samples recrystallized at $T = 1273$ K.

Comparison of the measured characteristics of corrosion resistance with the data on the microstructure of ion-doped layers suggests that the most probable mechanism for the enhancement of the corrosion resistance of the test steel after ion implantation is the reduction of the chemical activity of grain boundaries, first, due to the removal of harmful impurities during the formation of Y- or Ti-based interstitial phases; second, because of the increase in the relative area of these boundaries due to the decrease in grain size resulting from the suppression of accumulative recrystallization, and, third, owing to the prevention of the formation of coarse grain-boundary segregates of chromium carbides which plays an important role in the activization of intercrystalline corrosion in austenitic steels. The enhancement of the resistance of the test steel against ICC upon ion implantation of yttrium and titanium is also supported by the considerably reduced etchability of grain boundaries in the ion-doped samples in the process of their boiling in nitric acid.

As a result of the investigations performed, a method has been proposed for increasing the resistance of a material (steel 02X17H14M2) used for fuel element cans against intercrystallite corrosion in the active medium of the cooling agent. The method is realized in two steps:

ion implantation of yttrium or titanium;

annealing of ion-doped samples at 1273 K.

The proposed treatment conditions and ion implantation modes are the following:

Prior to ion implantation, the steel should be in the strained state at the stage, for fuel element cans, preceding the final thermal treatment.

The ion implantation is effected on type TITAN or MEVVA implanters evacuated by cryogenic pumps to a vacuum of $(2–4)\cdot10^{-6}$ Torr.

Accelerating voltage: ~50 kV.

Irradiation dose: $\sim10^{16}$ cm^{-2}.

References

[1] *High-temperature Mechanical Properties of Corrosion-Resistive Steels for Nuclear Energy Technology. Conference proceedings*, Ed. by G.N. Mekhed, Moscow, Metallurgia, 1987. (Mechanical Behaviour and Nuclear Application of Stainless Steel at Elevated Temperatures. Proceedings of the international conference, Villa Ponti, Varese, Italy on 20 – 22 May 1981, The Metal London Society.)

[2] *The Third Interindustry Conference on Reactor Material Science*, Dimitrovgrad, 27–30 October, 1992. Conference Proceedings. V. 1, 2, Dimitrogvrad, 1994.

[3] *The Fifth Interindustry Conference on Reactor Material Science*, Dimitrovgrad, 8–12 September, 1997. Conference Proceedings. V. 1, 2. Dimitrovgrad, 1998.

[4] S.A. Averin, V.A. Safonov, and M.I. Solonin, Ibid., Seria: Fizika Radiatsionnykh Povrezhdenii i Radiatsionnoe Metallovedenie **3**(54), 62 (1990).

[5] A.H. Tyumentsev, Yu.P. Pinzhin, A.D. Korotaev et al., Phase Nuclear Instruments and Methods in Physics Research **B80/81**, 491 (1993).

[6] A.D. Korotaev, A.N. Tyumentsev, S.P. Bugaev Structural-Phase Russian Physics Journal **37**, 452 (1994).

[7] A.D. Korotaev, A.N. Tyumentsev, Yu.P. Pinzhin et al., Surface & Coatings Technology **96**, 89 (1997).

[8] GOST (State Standard) 6032-84. *Electrochemical methods for determination of the resistance to intercrystallite corrosion*.

[9] M.A. Shluger, F.F. Azhogin et al., *Corrosion and Protection of Metals*, Moscow, Metallurgia, 1981.